



Fabrication and Characterization of Microfluidic Field Effect Transistor on Silicon Substrate

by

Maizatul binti Zolkapli

(0730110180)

A thesis submitted
in fulfillment of the requirements for the degree of
Master of Science (Microelectronic Engineering)

**School of Microelectronic Engineering
UNIVERSITI MALAYSIA PERLIS**

2010

**GRADUATE SCHOOL
UNIVERSITI MALAYSIA PERLIS**

PERMISSION TO USE

In presenting this thesis in fulfillment of a post graduate degree from Universiti Malaysia Perlis, I agree that permission for copying of this thesis in any manner, in whole or in part, for scholarly purposes may be granted by my supervisor or, in their absence, by Dean of the Graduate School. It is understood that any copying or publication or use of this thesis or parts thereof for financial gain shall not be allowed without my written permission. It is also understood that due recognition shall be given to me and to Universiti Malaysia Perlis for any scholarly use which may be made of any material from my thesis.

Requests for permission to copy or make other use of material in whole or in part of this thesis are to be addressed to:

Dean of Center for Graduate Studies

Universiti Malaysia Perlis

Jalan Bukit Lagi

01000 Kangar

Perlis Indera Kayangan

Malaysia

APPROVAL AND DECLARATION SHEET

This thesis titled Fabrication and Characterization of Microfluidic Field Effect Transistor on Silicon Substrate was prepared and submitted by Maizatul binti Zolkapli (Matrix Number: 0730110180) and has been found satisfactory in terms of scope, quality and presentation as partial fulfillment of the requirement for the award of degree of Master of Science (Microelectronic Engineering) in Universiti Malaysia Perlis (UniMAP).

Checked and Approved by

.....
(Associate Professor Dr. Prabakaran Poopalan)

School of Microelectronic Engineering

Universiti Malaysia Perlis

(Date:)

School of Microelectronic Engineering

Universiti Malaysia Perlis

2010

ACKNOWLEDGEMENTS

For the past two years I owe a lot to my advisory committee, my friends, my family and many others who had given me the confidence, and encouragement throughout those countless hard-working days and nights.

I am deeply grateful to my supervisor, Assoc. Prof. Dr. Prabaharan Poopalan. His wide knowledge, serious research attitude and enthusiasm in work deeply impressed me and taught me what a true scientific researcher should be.

My friends in photonic and failure analysis lab not just helped me with my research work, but also let me enjoy a friendly work environment. Amongst them, I would like to specifically thank Najah, Saziela, Ikhwan, Sutikno, Seng Fatt and Emi, from whom I learned a great deal when I was starting my research work. Many thanks also goes out to Steven, Mydin, Fizah, Gium, Bojie, Charan, Aladdin and many others that I cannot enumerate here for their endless moral support.

I am also grateful to the late Mr Phang and his team, Hafiz, Bahari, Shila and Hamidah who meticulously kept the research clean room functioning well at all times.

Finally my sincere appreciation to my husband Iesh, my two wonderful kids Sara and Raziq, and not forgetting Mak, Abah, Andong, Mak Long and my brothers for their love and support throughout these years. Only with their love and encouragement was this dissertation made possible.

TABLE OF CONTENTS

	PAGES
DECLARATION OF THESIS	ii
COPYRIGHT	iii
APPROVAL AND DECLARATION SHEET	iv
ACKNOWLEDGEMENTS	v
TABLE OF CONTENTS	vi
LIST OF TABLES	x
LIST OF FIGURES	xi
LIST OF ABBREVIATIONS	xvi
LIST OF SYMBOLS	xviii
LIST OF PUBLICATION	xix
ABSTRAK	xx
ABSTRACT	xxi

CHAPTER

1 INTRODUCTION

1.1	Introduction	1
1.2	Microfluidics and microfluidic devices	1
1.3	Survey of past experimental work	3
1.4	Microfluidic Field Effect Transistor	8
1.5	Objectives of this study	10
1.6	Dissertation Organization	10

CHAPTER

2 THEORY

1	Introduction	11
2	Metal Oxide Semiconductor Field Effect Transistor (MOSFET)	12
	N-channel Enhancement-type MOSFET	13
	Basic Structure	13
	Basic Operation and Characteristics	14
	2.2.2 N-channel Depletion-type MOSFET	16
	Basic Structure	16
	Basic Operation and Characteristics	17
3	Microfluidic Field Effect Transistor	19
	Basic Structure	19
	Basic Operation and Characteristics	20
4	Summary	24

CHAPTER

3 FABRICATION AND CHARACTERIZATION

	Introduction	25
	Photomask Design	26
	3.2.1 Alignment Mark Design	28
	3.2.2 Source and Drain Mask Design	29
	3.2.3 Channel and Reservoir Mask Design	30
	3.2.4 Contact Mask Design	30
	3.2.5 Holes for Gate Cover Mask Design	31
	3.2.6 Complete Mask Design	31
	Fabrication Process	32
	3.3.1 Wafer Preparation	33
	3.3.2 Oxidation	35

	3.3.3	Photolithography	36
3.3.3.1		Photoresist Coating and Soft Baking	36
3.3.3.2		Alignment and Exposure of Photoresist	37
3.3.3.3		Development of Patterns	37
3.3.3.4		Hard Baking	38
3.3.3.5		Pattern Inspection	38
	3.3.4	Etching	39
	3.3.5	Doping and Diffusion	41
	3.3.6	Physical Vapour Deposition (PVD)	42
	3.3.7	Gate Formation	42
		Electrical Testing and Characterization	44
		Summary	49
CHAPTER			
4 RESULT AND DISCUSSION			
		Introduction	51
		Wafer Preparation	51
		Thermal Oxidation	52
		Channel and Reservoir Formation	54
	4.4.1	Photolithography Channel and Reservoir	55
	4.4.2	Silicon Dioxide Etch at Channel and Reservoir Region	57
	4.4.3	Silicon Etch at Channel and Reservoir Region	58
	4.5	Source and Drain Formation	62
	4.5.1	Photolithography of Source and Drain	63
	4.5.2	Silicon Dioxide Etch at Source-Drain Region	64
	4.5.3	Phosphorus Doping and Diffusion at Source-Drain Region	65
	4.6	Exposing Silicon at Channel-Reservoir Region	66
	4.6.1	Photolithography of Channel-Reservoir	67
	4.6.2	Silicon Dioxide Etch at Channel-Reservoir Region	68
	4.7	Metallization	69

4.7.1	Aluminum Sputtering Using Plasma Vapor Deposition (PVD)	70
4.7.2	Photolithography of Contact	71
4.7.3	Aluminum Etch and Photoresist Strip	72
4.8	Gate Formation and Complete Device	73
4.9	Electrical Testing and Characterization	73
4.9.1	Source and Drain Resistivity	73
4.9.2	Current-Voltage (I-V) Characteristics	75
4.10	Summary	87

CHAPTER

5 CONCLUSION

Introduction	89	
Conclusion	89	
5.2.1	Fabrication of Microfluidic FET	89
5.2.2	Electrical Test Set-up of Microfluidic FET	92
5.2.3	Test and Characterization of Microfluidic FET	94
Recommendation for Future Work	96	

REFERENCES	98
-------------------	-----------

LIST OF TABLES

TABLES	TITLE	PAGES
Table 2.1	Summary of the enhancement and depletion type of MOSFET	12
Table 3.1	The silicon wafer specifications	33
Table 3.2	Summary of the wet etch processes	40
Table 3.3	Sample of tabulated data	46
Table 4.1	Results of starting material	51
Table 4.2	Optimized parameters for photolithography process	56
Table 4.3	Channel width measured with micrometer scale post photolithography process	57
Table 4.4	Channel width measured with micrometer scale post SiO ₂ etching process	58
Table 4.5	Channel width and depth measured with profilometer and SEM	60
Table 4.6	Channel resistance (between source and drain) of the microfluidic FET with and without DI water	74
Table 4.7	Summary of electrical test results	88

LIST OF FIGURES

FIGURE	TITLE	PAGE
Figure 1.1	Schematic of a nanofluidic transistor	4
Figure 1.2	Micrograph of the fabricated device, with 120 μ m long channels (scale bar is 10 μ m)	5
Figure 1.3	Illustration and realization of a microfluidic-based NOT gate	6
Figure 1.4	Fabricated flux stabilizer (non-linear resistor)	7
Figure 1.5	Microfluidic flip-flop	7

Figure 1.6	Two distinct flow patterns representing the states of the flip flop	8
Figure 1.7	Microfluidic FET overview showing the electrical contacts and source/ drain doped area (shaded). The clear areas indicate the reservoirs and channel	9
Figure 2.1	Physical structure of a typical <i>n</i> -channel MOSFET transistor	11
Figure 2.2	(a) <i>n</i> -channel enhancement type MOSFET, (b) circuit symbol	14
Figure 2.3	Channel formation in the <i>n</i> -channel enhancement-type MOSFET	14
Figure 2.4	Transfer and drain characteristics of <i>n</i> -channel enhancement-type MOSFET	16
Figure 2.5	(a) <i>n</i> -channel depletion type MOSFET, (b) circuit symbol	17
Figure 2.6	<i>n</i> -channel depletion-type MOSFET with $V_{GS} = 0V$ and an applied voltage V_{DD}	17
Figure 2.7	Reduction in free carriers in channel due to a negative potential at the gate terminal	18
Figure 2.8	Transfer and drain characteristics of <i>n</i> -channel depletion-type MOSFET	19
Figure 2.9	Schematic representation of microfluidic transistor	20
Figure 2.10	Schematic of an electroosmotic flow channel with a finite EDL. The charges drawn in the figure indicate net charge. The boundary layers on either wall have a thickness on the order the Debye length of the solution	21
Figure 2.11	Cross section of microfluidic FET with (a) positive gate voltage applied and (b) negative gate voltage applied	22
Figure 3.1	Top-down microfabrication method	26
Figure 3.2	A 100 mm diameter circle is divided into four quadrants	27
Figure 3.3	Alignment mark with dimensions; (a) Alignment mark for layer 1 and 3 placed at the edge of the wafer, (b) Alignment mark for layer 2 and 4 placed at the edge of the wafer and (c) Center alignment mark for all four layers	28
Figure 3.4	A complete alignment mark on a piece of glass mask	29
Figure 3.5	Source and drain dimension	29
Figure 3.6	The dimension of channel and reservoir structure with <i>x</i> varies between 5 μm to 500 μm	30
Figure 3.7	Contact dimension	30
Figure 3.8	Gate holes dimension	31
Figure 3.9	(a) A complete mask set for microfluidic FET fabrication and (b) The schematic representation of the microfluidic transistor	32
Figure 3.10	The process flow for the fabricated device	33
Figure 3.11	Thickness of the microscope cover slip measured using	43

	profilometer	
Figure 3.12	Top view of the completed microfluidic FET	44
Figure 3.13	Keithley 4200 Test Environment Setup for resistance test	44
Figure 3.14	The circuit configuration for microfluidic FET manual testing	45
Figure 3.15	Manual test connection for microfluidic FET IV characteristic	47
Figure 3.16	Close up of the sample connection	47
Figure 3.17	Hot spot at source and drain	48
Figure 3.18	IRF640 IV curve from SPA	48
Figure 3.19	IRF640 IV curve from manual test circuit	49
Figure 3.20	IRF640 IV curve from Tektronix 370B curve tracer	49
Figure 4.1	Graph of the native oxide thickness of the starting material before and after 30 seconds BOE	52
Figure 4.2	Graph of SiO ₂ thickness against oxidation time	53
Figure 4.3	Graph of SiO ₂ thickness after 6 hours oxidation. Oxide layer protects channel and reservoir region during doping and diffusion process	54
Figure 4.4	Schematic diagram of the steps involved in the channel and reservoir formation (layer thickness not to scale): (a) the mask is being exposed under I-line, 365 nm UV light for pattern transfer, (b) develop PR to wash away the non-reacted polymer, (c) etching SiO ₂ to open up silicon area, (d) resist removal, (e) silicon etch (30 wt% KOH at 80 °C) and (f) dry oxidation to protect channel and reservoir during source-drain diffusion	55
Figure 4.5	HPM images of the various channel width after the developing process. The patterned are well defined and the size matches the drawn design	56
Figure 4.6	HPM images of the various channel width after the 1 hour BOE. SiO ₂ is removed in the reservoir and channel region	58
Figure 4.7	HPM images of the various channel width post KOH etch	59
Figure 4.8	Profilogram of the channel width and depth. On the left is the channel width and on the right is the channel depth for (a) 5 μm channel, (b) 20 μm channel, (c) 50 μm channel, (d) 100 μm channel and (e) 500 μm channel respectively	61
Figure 4.9	SEM micrographs of the channel width and depth after KOH etching using 30 % concentrated etchant for 12 minutes at 80 °C. The anisotropic wet-etched profile in <100> wafer is shown	62

Figure 4.10	Schematic diagram of the steps involved in the source and drain formation (layer thickness not to scale): (a) the mask is being exposed under I-line, 365 nm UV light for pattern transfer, (b) develop PR to wash away the non-reacted polymer, (c) etching SiO ₂ to open up silicon area and (d) phosphorus doping and diffusion at source and drain region	63
Figure 4.11	Aligning the source-drain mask at the centre of the existing channel-reservoir	63
Figure 4.12	Misalignment of second layer to the first layer. The source-drain and channel are not touching	64
Figure 4.13	HPM images of source/drain structure aligned to the channel after developing	65
Figure 4.14	Lower sheet resistance post diffusion indicates dopant have diffused through the silicon. The processing time is 30 min	66
Figure 4.15	Schematic diagram of the steps involved to remove SiO ₂ at the channel-reservoir area (layer thickness not to scale): (a) the mask is being exposed under I-line, 365 nm UV light for pattern transfer, (b) develop PR to wash away the non-reacted polymer, (c) etching SiO ₂ to open up silicon area at channel-reservoir region	66
Figure 4.16	Misalignment of PR and existing pattern	67
Figure 4.17	Patterns are properly aligned and the oxide at the channel-reservoir region is ready to be etched away	68
Figure 4.18	Channel-reservoir posts 12 minutes BOE etch. Colour changed from pink to grey	69
Figure 4.19	Schematic diagram of the steps involved in the metallization process: (a) Aluminum is deposited on the sample, (b) the mask is being exposed under I-line, 365 nm UV light for pattern transfer, (c) develop PR to wash away the non-reacted polymer, (d) etching aluminum for metallization	70
Figure 4.20	The profilogram for aluminum thickness after three deposition process	70
Figure 4.21	Sample surface after aluminum deposition process	71
Figure 4.22	Contact at source-drain region after photoresist developed process	72
Figure 4.23	Contact region after aluminum etch and photoresist strip	72

Figure 4.24	The completed structure of the microfluidic FET	73
Figure 4.25	SPA plots for channel resistance	74
Figure 4.26	Measuring resistivity between source and drain for both with and without liquid in the channel	75
Figure 4.27	I-V plot for 20 μm channel, positive and negative V_{GS} with different V_{DS} for (a) dry test and (b) wet test	77
Figure 4.28	I-V plot for dry test, positive and negative V_{GS} for (a) 5 μm , (b) 20 μm and (c) 50 μm channel	79
Figure 4.29	I-V plot for wet test, positive and negative V_{GS} for (a) 5 μm , (b) 20 μm and (c) 50 μm channel	81
Figure 4.30	I-V curves of 5 μm channel comparing dry and wet test by (a) applying positive V_{GS} and (b) applying negative V_{GS}	83
Figure 4.31	I-V curves of 20 μm channel width comparing dry and wet test by (a) applying positive V_{GS} and (b) applying negative V_{GS}	84
Figure 4.32	I-V curves of 50 μm channel width comparing dry and wet test by (a) applying positive V_{GS} and (b) applying negative V_{GS}	86
Figure 4.33	I-V curve comparing different channel widths for dry and wet for a fixed V_{DS} (4 V)	87
Figure 5.1	The circuit configuration for microfluidic FET manual testing	93
Figure 5.2	IRF640 IV curve from SPA	93
Figure 5.3	IRF640 IV curve from manual test circuit	94
Figure 5.4	IRF640 IV curve from Tektronix 370B curve tracer	94

LIST OF ABBREVIATIONS

Al = Aluminum

© This item is protected by original copyright

BJT	=	Bipolar Junction Transistor
BOE	=	Buffered Oxide Etch
CTA	=	Conventional Thermal Annealing
DIW	=	De-ionized Water
DNA	=	Deoxyribonucleic Acid
EDL	=	Electrical Double Layer
FET	=	Field Effect Transistor
HPM	=	High Power Microscope
ICP-RIE	=	Inductive Coupled Plasma-Reactive Ion Etching
KITE	=	Keithley Interactive Test Environment
KOH	=	Potassium Hydroxide
MEMS	=	Microelectromechanical Systems
MOSFET	=	Metal Oxide Semiconductor Field Effect Transistor
MOSol	=	Metal-oxide-solution
NMOS	=	N-channel Metal Oxide Semiconductor
OFM	=	Oxidation Furnace Module
PECVD	=	Plasma Enhancement Chemical Vapour Deposition
PR	=	Photoresist
PVD	=	Physical Vapour Deposition
RCA	=	Radio Corporation of America
SC	=	Standard Cleaning
SEM	=	Scanning Electron Microscope
Si	=	Silicon
SiO ₂	=	Silicon dioxide
SMU	=	Source Monitor Units
SOG	=	Spin On Glass
SPA	=	Semiconductor Parametric Analyzer
UV	=	Ultraviolet
WCM	=	Wet Cleaning Module
μTAS	=	Miniaturized Total Chemical Analysis System
+ve	=	Positive
-ve	=	Negative

LIST OF SYMBOLS

Quantity	Symbol	Unit
Drain current	I_D	Ampere (A)
Drain voltage	V_{DS}	Volts (V)
Gate voltage	V_G	Volts (V)
Load resistance	R_L	Ohm (Ω)
Load resistance voltage	V_L	Volts (V)
Sheet resistance	R_s	ohms per square (Ω/\square)

LIST OF PUBLICATION

1. M. Zolkapli, N.M. Zabidi, V. Retnasamy, Z. Sauli, and P. Poopalan. Fabrication of Microfluidic Transistor on Silicon Substrate. 2009 International Symposium on Electrohydrodynamics.

**FABRIKASI DAN PENCIRIAN TRANSISTOR KESAN MEDAN BENDALIR
MIKRO DI ATAS SUBSTRAT SILIKON**

ABSTRAK

Pembinaan transistor kesan medan pengaliran bendalir mikro berasaskan silikon telah dijalankan. Objektif utama kajian ini dijalankan adalah untuk mempersembahkan daripada konsep, rekabentuk transistor kesan medan pengaliran bendalir mikro dan menghasilkan aliran proses yang berkaitan dalam fabrikasi transistor kesan medan bendalir mikro di atas kepingan silikon, yang akhirnya akan diperincikan menggunakan ujian-ujian yang bersesuaian. Maka, fabrikasi di atas silikon jenis p-<100> bersaiz 4 inci melalui proses fotolitografi, hakisan secara kimia, pengoksidaan termal, penyesaran dan pelogaman dengan focus khususnya ke atas laluan konduksi bendalir telah dijalankan. Tiga peringkat topeng foto telah direkabentuk menggunakan perisian AUTO-CAD dan dicetak krom di atas kaca jenis soda-kapur. Struktur asas peranti ini telah diadaptasi daripada struktur MOSFET sedia ada dan telah diolah untuk menggabungkan laluan bendalir di dalam operasinya. Oleh itu, tiada perubahan dari segi fungsi tetapi laluan konduksi utama diganti dengan bendalir, dan bukannya semikonduktor yang telah didopkan. Dua tangki dihubungkan melalui satu laluan bendalir dengan setiap satu kawasan punca dan saliran yang telah didopkan diletakkan di kedua-dua bahagian yang bertentangan dengan laluan bendalir untuk mengurangkan konduksi terhadap substrat. Kedua-duanya diletakkan jauh antara satu sama lain bagi meminimakan pengaliran elektron melalui laluan bendalir bilamana aliran tersebut tidak diisi dengan cecair. Lebar aliran telah ditetapkan kepada lima saiz, iaitu 5 μm , 20 μm , 50 μm , 100 μm dan 500 μm untuk mengkaji kesan ke atas pencirian transistor berbanding saiz aliran. Mobiliti

elektron di dalam laluan bendalir terkesan dengan kehadiran cecair polar. Halaju elektron kini mengalami lebih banyak pelanggaran dengan molekul air yang bergerak dan polar, disertai dengan kesan medan elektrik yang dikenakan pada get. Profil laluan bendalir diperiksa dengan bantuan stilus profilometer dan SEM. Isu penutupan get di atas laluan bendalir diatasi dengan menggunakan satu lapisan kaca nipis yang telah disalut dengan aluminium pada sebelah permukaannya dan dilekatkan ke atas permukaan silikon. Tetapi teknik tersebut akan menyebabkan lebih tinggi ambang voltan kerana tebal silika ialah $80\ \mu\text{m}$ dan jauh lebih tebal berbanding oksida MOSFET yang biasa. Kebiasaannya tebal lapisan oksida MOSFET adalah di sekitar $0.02 - 0.1\ \mu\text{m}$. Justeru, ia akan menyebabkan pengurangan medan elektrik di sekitar kawasan get. Ujian ke atas peranti berlansung semasa proses fabrikasi, di mana pelbagai kerintangan, ketebalan lapisan yang dihasilkan dan parameter-parameter lain diukur. Namun, ukuran-ukuran tersebut tidak dapat memberi pengertian atau pemahaman kepada prestasi akhir peranti tersebut. Oleh yang demikian, ujian elektrik dilaksanakan bagi kedua-dua kondisi iaitu dengan dan tanpa cecair di dalam laluan bendalir dengan menggunakan alat penganalisa parametrik semikonduktor, penyurih lengkung dan litar berarus tinggi. Pencirian I-V dan kerintangan peranti dianalisa dan keputusan menunjukkan terdapat hubungan di antara arus dan voltan serta cirinya mematuhi teori. Namun demikian, peranti ini tidak dapat dikategorikan sebagai PMOS atau NMOS kerana laluan bendalir tidak didopkan. Keputusan menunjukkan rintangan berkurangan sebanyak satu tingkat bagi kondisi basah berbanding kondisi kering. Ini sekali lagi menunjukkan kehadiran molekul air di dalam laluan bendalir membantu memperbaiki mobiliti pengangkut.

© This item is protected by ORCID iD

FABRICATION AND CHARACTERIZATION OF MICROFLUIDIC FIELD EFFECT TRANSISTOR ON SILICON SUBSTRATE

ABSTRACT

The development of a silicon-based microfluidic field effect transistor has been carried out. The main objective of this study is to present from concept, the design of a microfluidic FET and to develop its appropriate process flow in fabricating the microfluidic FET on silicon wafer, which will finally be characterized using a suitable test methodology. Hence, fabrication on a p- $\langle 100 \rangle$ 4 inch silicon wafer by photolithography, wet chemical etching, thermal oxidation, diffusion and metallization with focus on a liquid conduction path has been executed. A three level photo mask has been designed via AutoCAD and chrome printed on soda-lime glass. The basic structure of the device is adapted from the conventional MOSFET structure and redesigned to incorporate a liquid channel in its operation. Therefore, the functionality remains unchanged but the principal conduction path is replaced by a fluid instead of a doped semiconductor. Two reservoirs are connected via a channel with source and drain regions doped on opposite sides of the liquid channel to reduce conduction through the substrate. They are placed as far away from each other in order to minimize electron flow through the fluidic channel when not filled with fluid. The channel widths are set to five sizes, which are 5 μm , 20 μm , 50 μm , 100 μm and 500 μm in order to study the effect of the transistor characteristics against channel size. The electron mobility in the channel is significantly affected due to the presence of polar liquid. The electron drift velocity now undergoes more collisions with mobile water molecules, which is itself polar and hence affected by the applied gate electric field. The channel profiles are inspected with the aid of stylus profilometer and SEM. The capping issue of the gate on the channel i.e. a void is addressed using a thin layer of single-side aluminum coated glass glued onto the silicon surface. This however results in higher threshold voltage as the silica thickness is about 80 μm , which is much thicker than the normal MOSFET oxide. Typically the thickness of the oxide layer in MOSFET is in the range of 0.02 - 0.1 μm . Therefore, this causes higher reduction in electric field at the gate area. Testing of the devices commences during the fabrication process where the various resistivity, grown layer thicknesses and other parameters are measured. However, these measurements do not give an insight towards the final device performance. Thus, an electrical test is performed on both conditions, with and without liquid inside the channel using the semiconductor parametric analyzer, curve tracer and a high current circuit. I-V characteristics and resistivity of the devices is analysed and the results show that there is some current and voltage relation and the characteristics does conform to the theory. However, the device can not be categorized either as PMOS or NMOS since the channel is undoped. The resistance is reduced by one order for wet condition as compared to dry condition. This again shows that the presence of water molecules in the channel improves the carrier mobility.

CHAPTER 1

INTRODUCTION

1.1 Introduction

The semiconductor industry has grown rapidly in the past few decades, driven by the microelectronics revolution. New technologies emerge with new materials and manufacturing processes that are used to create new products. Microelectronic processing has also fuelled integrated microfluidic systems which have gained interest in recent years for many applications including chemical, medical, automotive and industrial (Gad-el-Hak, 2006, p. 3-1). This chapter provides the background knowledge on which the studies are based.

1.2 Microfluidics and microfluidic devices

Microfluidics is a multidisciplinary field comprising of physics, chemistry, engineering and biotechnology which deals with the behavior, precise control and manipulation of microliter and nanoliter volumes of fluids. It has been an area of intense research, where the key aspect of microfluidics is its smallness. This attribute brings new elements which are not only quantitative, but also qualitative (Ottino & Wiggins, 2004; Karnik, Castelino & Majumdar, 2006).

The volumes involved in microfluidics can be understood by visualizing the size of a one-litre container, and then imagining cubical fractions of this container. A cube measuring 100 mm on an edge has a volume of one litre. A tiny cube whose height, width and depth are 1/1000 (0.001) of this size or 0.1 mm is the size of a small grain of table sugar. That cube will occupy 1.0 nl. A volume of 1.0 pl is represented by a cube

whose height, width and depth are 1/10 (0.1) of the 1.0 nl cube. It would thus take a powerful microscope to resolve this size.

Microfluidic devices on the other hand, are devices where micron sized fluid channels fabricated on a suitable substrate to achieve a specific end application. Channels of the micro-devices are mostly silicon, glass, or quartz based and is fabricated by photolithography, etching, deposition, microwetting, and microimpression which permit the fabrication of miniaturized systems. Interconnection of channels allows the realization of networks along which liquids can be transported from one location to another on a device surface. In this way, small volumes of solution may be introduced from one channel into another, and controlled interaction of reactants is made possible (Verpoorte & Rooij, 2003). Other than channels, nozzles, pumps, mixers, valves, filter, sensors are also categorized as microfluidic devices (Permal, 2007). Typically these devices are either static or increasingly dynamic where the liquid flows through the channels and bends. The small size of the channels combined with capillary effects, pump effects (if any pump is used) and bend effects enable separation and subsequent identification of minute quantities of elements. The ability to manipulate fluids at the micron level brings in several advantages (Marr & Murakata, 2007):

1. A significant reduction of sample consumption.
2. A larger number of devices consisting of hundreds to thousands of channels and valves can be incorporated on a small planar surface allowing simultaneous parallel and complex analyses.
3. Smaller processing time for analyses and synthesis that can be done at the point of need than at a centralized laboratory (bringing laboratory to the sample).
4. The fabrication methods are based on traditional silicon-based technologies

which make them easier and cheaper to produce.

Fabrication of microfluidic devices presents new challenges for micro- and nano-engineering. With increasing demand for products associated with the medical, pharmaceutical, and analytical science industries over the past few years, much attention has been paid to the design and manufacture of microfluidic devices. Intensive research has been made especially on silicon-based microfluidic devices (Jackson, 2006). Silicon has become the material of choice for most microfluidic applications because of the well-explored microfabrication techniques of silicon itself. It makes the combination of the mechanical and electrical function in single devices possible (Verpoorte & Rooij, 2003) providing the impetus in the area of MEMS for the enormous activity over the past three decades.

Since the establishment of the field of μ TAS in 1990 by Manz, Graber and Widmer, device design and process integration remains as an interesting challenge to be solved (Manz, Graber & Widmer, 1990). In this study, the focus is directed towards the fabrication technology and its related characterization which allows the realization of a silicon-based microfluidic field effect transistor.

1.3 Survey of past experimental work

From as early as 1960s, fluidic systems have been experimented with, to perform logic operations. Erickson and Li (2003) reported that modern microfluidics (Gravesen, Branebjerg & Jensen, 1993) can be traced back to the development of a silicon chip based gas chromatograph at Stanford University and the ink-jet printer at IBM. Though both these devices were quite remarkable, the concept of the integrated microfluidic device (which often fall under the broad categories of labs-on-a-chip or miniaturized total analysis systems) as it is known today was not developed until the

early 1990s by Manz, Graber and Widmer (1990) (Erickson & Li 2004). Since that time the field has blossomed and branched off into many different areas, for which a number of excellent general reviews are available such as biological and chemical analysis (Jakeway, de Mello & Russell, 2002; Beebe, Mensing & Walker, 2002; Chovan & Guttman, 2002), point-of-care testing (Tüd"os, Besselink & Schasfoort, 2001), clinical and forensic analysis (Verpoorte, 2002), molecular diagnostics (Huang, Mather, Bell & Madou, 2002) and medical diagnostics (Vo-Dinh & Cullum, 2000).

It is a new science, having emerged only in the 1990s, therefore the number of applications for this technology is currently small. The most mature application of microfluidics technology is ink-jet printing, which uses orifices less than 100 μm in diameter to generate drops of ink. Today, ink-jet printing is moving out of the office and into biotechnology to deliver reagents to microscopic reactors and deposit DNA into arrays on the surface of biochips (Ouellette, 2003).

A closest work related to this study but in a nano regime led by Dr. Majumdar and Dr. Yang from University of California, Berkeley is the nanofluidic transistors which control the flow of ions through nano-scaled water-filled tubes (Karnik, Fan, Yue, Li, Yang & Majumdar, 2005). Figure 1.1 shows a schematic diagram of the constructed nanofluidic transistor.

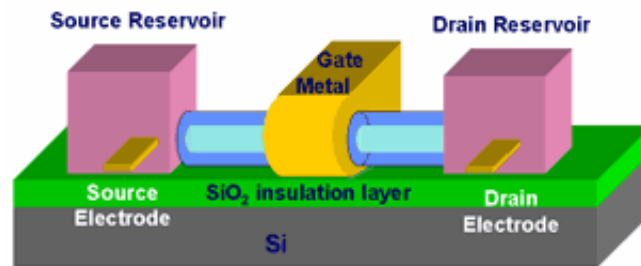


Figure 1.1: Schematic of a nanofluidic transistor (Karnik, Fan, Yue, Li, Yang & Majumdar, 2005).